A Novel Approach to Quantification of Real and Artifactual Components of Current Density Imaging for Phantom and Live Heart

F. H. Foomany[1], M. Beheshti[1], K. Magtibay[1], S. Masse[2], P. Lai[2], J. Asta[2], N. Zamiri[2], D. A. Jaffray[3], S. Krishnan[1], K. Nanthakumar[2], and K. Umapathy[1]
Ryerson University[1], Toronto General Hospital[2], Princess Margaret Hospital[3]

***Abstract*— Spatial distribution of injected current in a subject could be calculated and visualized through current density imaging (CDI). Calculated CDI paths however have a limited degree of accuracy due to both avoidable methodological errors and inevitable limitations dictated by MR imaging constraints. The source and impact of these limitations are scrutinized in this paper. Quantification of such limitations is an essential step prior to passing any judgment about the results especially in biomedical applications. An innovative technique along with metrics for evaluation of range of errors using baseline and phase cycle MR images is proposed in this work. The presented approach is helpful in pinpointing the local artifacts (areas for which CDI results are suspect), evaluation of global noises and artifacts and assessment of the effect of approximation algorithms on real and artifactual components. We will demonstrate how this error/reliability evaluation is applicable to interpretation of CDI results and in this framework, report the CDI results for an artificial phantom and a live pig heart in Langendorff setup. It is contended here that using this method, the inevitable trade-off between details and approximations of CDI components could be monitored which provides a great opportunity for robust interpretation of results. The proposed approach could be extended, adapted and used for statistical analysis of similar methods which aim at mapping current and impedance based on magnetic flux images obtained through MRI.**

I. Introduction

A. Motivation and Problem Definition

Low frequency current density imaging (LF-CDI) allows calculation of paths of an injected current in a subject using MRI phase images [1, 2]. In LF-CDI current is passed through an MRI safe subject in a specific fashion in two phase cycles [3]. It could be shown that passing current in that manner does not affect MR magnitude images but the phase of the MR-images will have an additional component (extra to baseline phase) which is proportional to the magnetic flux. This is well documented in [2]. Since MRI only measures magnetic flux in one dimension, to calculate three components of magnetic flux, the subject needs to be rotated twice. Avoiding these rotations has motivated some approximations towards single-component CDI [6] though in general it is known that current cannot be uniquely established using only one component of magnetic flux [8]. One of the main applications of CDI resides in analysis of electrical characteristics of tissues. Several works have shown use of CDI as a non-invasive method for measurement of current distribution in tissues. Those include CDI of chicken femur bone [9], various organs of live pig [10], mice tumor [12] and post-mortem pig heart [14]. The phase images and therefore results of CDI could be noisy, regionally sporadic (as shown here) and generally spiky as shown in [7, 12]. There is a global pattern created by the current and a superimposed fluctuation of current whose validation requires further analysis. Sensitivity of CDI to noise and artifacts has not been overlooked in the past. A strong analysis of CDI sensitivity to various factors is offered in [15]. It is observed that different types of noises could appear in MRI phase images such as salt and pepper noise [7] and Gaussian noise [13]. Magnitude images in MRI receive a noise with Rice distribution while the phase images noise distribution tends to be uniform for low-magnitude points and zero mean Gaussian for high-magnitude points [13]. Since CDI is based on gradient of images in two directions the noise effect is exacerbated which results in highly fluctuating current values. In [16] a few criteria for discarding 'poor quality measurements' was suggested which indicated that combining all the criteria qualified less than 2% of high SNR points as high quality. A CDI reliability metric based on Gauss's law of magnetism was proposed in [14]. Aside from noises, the artifacts are also present in MRI phase images e.g. due to susceptibility variations [5, 17, 18]. To alleviate the effect of noises and artifacts on phase images many approaches are tenable for example ramp-preserving de-noising algorithm was recently suggested [7]. The gist of above discussion is that CDI has biomedical applications in which we need to compare current pathways in different situations. Noises, artifacts and matching requirements of CDI affect calculated current maps. On one hand we need compensation algorithms to improve the results and on another a method to assess the impact of such algorithms on true and artifactual components of CDI is required.

B. Contribution of this Work and Proposed Solution

This work offers a method for evaluation of CDI reliability. The core idea is that we propose measuring a baseline phase image (no current), passing current in phase cycle 1, passing current in phase cycle 2 (opposite current) and optionally measuring a second baseline phase (no current) for each orientation. Using this data allows shaping a hypothesized baseline (by adding two phase cycles) in addition to measured baseline which enables analysis of noises and artifacts and offers a metric for evaluation of range of reliability and errors in CDI. In this framework we

Resrach funded and supported by CIHR (grant number: 111253).

evaluate some of the hypotheses and report interesting results about a phantom and a live heart CDI experiment.

I. Method

A. Current Density Imaging

In CDI, the magnetic flux created by induced current shows itself as phase in MRI images. This phase is related to the induced magnetic flux as follows [1, 2]:

$$\psi = \gamma \cdot B \cdot T_c \qquad (1)$$

where γ is gyromagnetic ratio, B is the induced magnetic flux (parallel to MRI main magnetic field), ψ represents the phase and T_c is total current pulse duration. By applying the Maxwell equation (Ampère's law) we can determine current density maps if having magnetic flux values. To eliminate various baseline effects, current is passed in two opposite phase cycles (PCs). The images are phase unwrapped to remove 2π phase discontinuities [3]. Subtraction of PCs which now represents 2 times magnetic flux is then derived and using Ampère's law the current paths are calculated. The derivatives of the phase images on the edges are unreliable and are eroded. Therefore the masks for orientations are combined and an erosion algorithm is applied on them.

B. Classification of Sources of Error

Table I is the result of close analysis of steps in CDI. Signal to noise ratio has a significant impact on choice of mask. There is always a trade-off in choosing the masking threshold. Unwrapping the images, centering the images, and smoothing of the images are all affected by the choice of mask. Combined with the erosion a strict mask threshold may cause loss of data in many areas. On the contrary, a permissive masking threshold causes error in centering images (mismatch among images) and spurious CDI values within masked areas (e.g. big spikes). A debatable assumption of CDI is that the current always passes the same path in repetitions and that the impedance of the subject will remain constant during the experiment. These assumptions could be evaluated using our proposed method.

C. Quantification of Hypothesized Baseline Error

Fig 1 displays the proposed method. As opposed to normal CDI, in baseline analysis CDI, two phase cycle phase images are added and divided by two. We will call this image hypothesized baseline. Hypothesized baseline is used as PC1 for CDI analysis while PC2 is the normal baseline. Normal CDI procedure is followed after this. If we measure two real baseline images we can also complete CDI analysis with two baselines as well to obtain 3 sets of CDI (normal CDI (NORM_CDI), two real baselines CDI (BAS_CDI) and real/hypothesized baseline CDI (HYP_CDI)). In ideal situation if signal acquisition was noiseless, images (PCs and orientations) were perfectly matched and current passed the same path (in repetitions), the result of last two analyses would be absolute zero. Accumulation of all these problems (failure to cancel currents in PC1 and PC2, different paths, fluctuation in images as a result of noises and stochastic characteristics) demonstrates itself in CDI baseline analysis. Based on profile of noises [13] we expect the noises to exhibit their effect in BAS_CDI and HYP_CDI as a zero-mean calculated current and a standard deviation which offers a range of reliability. Since CDI is linear (i.e. if current I1 creates set of MRI phases PH1 and I2, PH2, current I1+I2 creates PH1+PH2) this effect is additive on normal CDI as well. Therefore we can quantify the range of statistical variations in CDI. In addition, if we fail to match the images while we have some susceptibility artifacts, the failure will show itself in BAS_CDI. HYP_CDI is specifically designed to analyze the hypothesis about the same-current path. Comparison of HYP_CDI and BAS_CDI shows whether noises/artifacts are exacerbated by current or not. Finally we can see the effect of smoothing on the BAS_CDI and NORM-CDI to monitor the trade-off between details and approximation of calculated current.

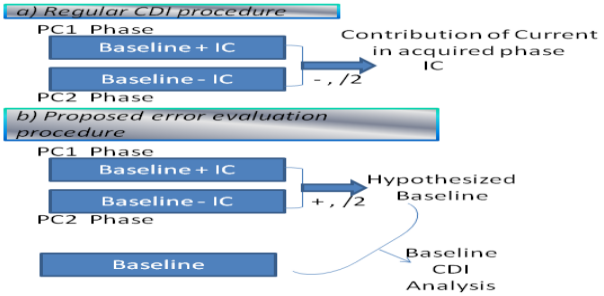

Fig 1. Proposed method for reliability evaluation (IC represents contribution of current in acquired phase images (PCs))

TABLE I. Sources of Error in CDI Calculation

Source of Error	Description/Note
MRI Signal Acquisition	Effect of various artifacts/noises on phase/magnitude images
Matching and Centering Images for PCs and Orientations	Matching the center of images (e.g.) based on masks could be imperfect.
Mask Erosion	When SNR is low several areas in image are masked out and eroded.
Same-Current Path	Assumption that current passes the same path in every repetition.
Smoothing	Which removes details about CDI

D. Measure of Fluctuation and Test of Hypotheses

We analyze a measure of fluctuation for baselines. In general we can fit a second order 2D polynomial surface (S) to the current density images (J) using linear least square method [19]. Then F will be the standard deviation of difference between surface and current density:

$$F = \sqrt{\frac{1}{N-1}\sum_{(x,y)\in M}(J(x,y)-S(x,y))^2} \qquad (3)$$

J is the current density values, N is the number of points in the mask, M is the set consisting of points in the mask and S

is the surface. *S* could be constructed based on a model-based assumption for current density, for example through ramp-fitting or polynomial fitting. In this work we only report fluctuation for baselines. Therefore we set *S* to the mean of the *J* which makes F the standard deviation of *J*. Alternatively we could set *S* to *0* for baselines.

E. Smoothing Current Density Images

We have evaluated several methods for smoothing CDI images. The first method used here applies a sliding window to the image that assigns the median of the window (for points inside the eroded mask) to each point. A second method utilized is Perona/Malik (PM) ramp preserving de-noising technique which is an iterative low pass filtering method that preserves the edges inside the image while smoothes out the rest of points through a diffusion differential equation [4]. Finally we show the results of CDI when a 2D polynomial surface of order 5 is fitted on CDIs.

F. Experimental Setup

We carried out phantom CDI experiment for a specifically designed phantom with two bars to simulate cavities in a subject. The MRI scan parameters were: image size of 256 by 256, field of view of 15 cm , number of excitations (NE) of 2, repetition time of 700 ms, echo time of 40ms, total current pulse width of 18ms (per slice) and slice thickness of 7mm for 6 slices. The injected current was 20mA. Voltage over a fixed resistor in series with phantom was read and saved on a digital oscilloscope. For the heart a novel mobile Langendorff setup was made to keep isolated pig heart alive. The pig heart is extracted based on Animal Use Protocol (AUP) from healthy pig under deep anaesthesia and it was performed in an Operation Room at the Animal Resource Centre of Toronto General Hospital

The passed current was about 25mA. The parameters were the same as for phantom except NE was 3. Prior to PM a mask-based median-filter of order 5 was applied on phase images to remove salt-pepper noise.

II. Results

Fig.2 shows the SNR for phantom and heart experiment calculated using magnitude-based MRI SNR equation [11]. The figure shows that SNR among baseline and phase cycles has not changed implying that current has not exacerbated the image quality. Our further inspection showed that it was signal strength that was lower for heart and the standard deviation of peripheral noise was in the same range for both experiments. Fig.3 displays 6 different CDIs (for 6 slices). From left: NORM_CDI, polynomial fitted NORM_CDI, BAS_CDI, HYP_CDI, NORM_CDI after PM applied on phases, BAS_CDI after PM applied on phases (all 5 point median filtered). It could be observed how the proposed method could serve as a visual tool for identifying the problematic areas: The centers of HYP_CDI and BAS_CDI have zero mean fluctuation. This fluctuation could be quantified as a measure of reliability and statistical analysis. On the top 2 slices however, you can see some artifacts (that could be because of not sustained susceptibility problem) that is not averaged to zero by smoothing. The artifact has not been constant and is not cancelled in BAS_CDI (we further analyzed the phase images and noted that it is present only in the first orientation and because of local movement of the artifact has not entirely been cancelled out).

Fig.4 demonstrates interesting results about heart and phantom CDI. The fluctuation for 6 slices is shown for BAS_CDI and HYP_CDI for heart and phantom for a 30 point circle in the center of each subject (to avoid artifacts). The analysis has been performed on images smoothed using 5 and 25 point mask-based smoothing algorithm. The fluctuation in CDI shows analogous for BAS_CDI and HYP_CDI which suggests that the fluctuation is not related to passing current. More interestingly, while generally the fluctuation in center area of heart is higher; it is still in the range of phantom fluctuation. It may imply that there is an additive fluctuation that is present in the phase images due to the inhomogeneity introduced by the tissue. First two slices have some artifact as could be seen in Fig. 4 thus show a lot of fluctuations as before mentioned. The fluctuation is reduced as the window for median filter becomes larger which is expected due to its zero mean. It shows that there is a trade-off between local/position information given by CDI and the clarity of images which could be quantified and monitored by baseline analysis.

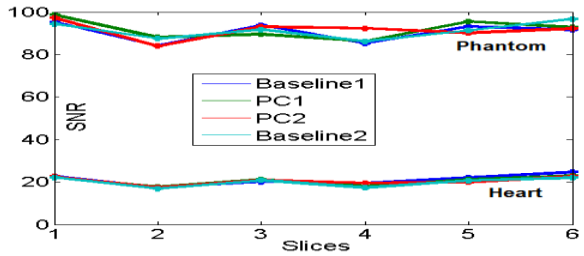

Fig. 2 SNR of MRI magnitude images

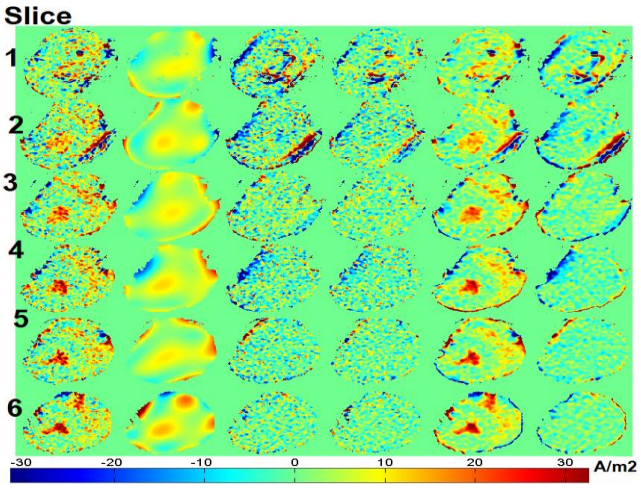

Fig. 3 Six slices of heart CDI, left to right: NORM_CDI, polynomial fitted NORM_CDI, BAS_CDI, HYP_CDI, NORM_CDI after PM applied on phases, BAS_CDI after PM applied on phases (all 5 point median filtered).

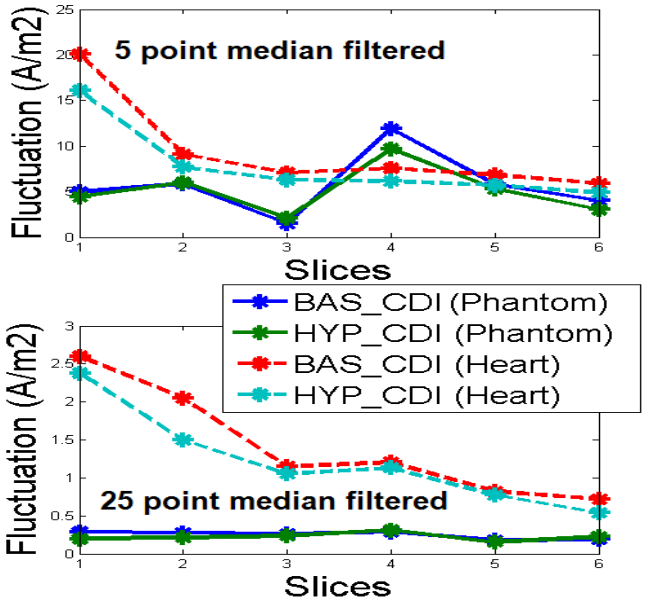

Fig. 4 Fluctuation for phantom /heart: BAS_CDI and HYP_CDI

III. Conclusion

A new method for analysis of range of reliability for CDI based on baseline images was proposed here which allowed study of accumulated noises, artifacts and post-processing errors. Although this study was dense with methods/results we strived to keep the central idea clear that the MR baseline images are extremely helpful to MR-based current evaluation methods (such as CDI and MR-EIT). It was observed that CD images might be noisy and sporadic which calls for a reliability analysis metric. We used a combination of PC1/PC2 and baseline to evaluate the range of methodological errors and noises. The phenomena underpinning CDI are stochastic and baseline analysis offers opportunity for quantitative analysis of statistics of phenomenon and therefore stochastic analysis of hypotheses about paths of currents. The current could be represented as an approximation plus/minus a range of the possible fluctuation in different locations. The method allows evaluation of statistical significance of difference between two instances of current, passed in two different statuses of heart. We also reported some of our findings in this framework which were important for further study of heart characteristics using CDI. The proposed technique offers a strong tool for analysis and interpretation of CDI results and could be treated as a tool for CDI reliability analysis.

IV. Acknowledgment

The authors would like to thank Mr. Eugen Hlasny and Mr. Neil Spiller from Toronto General Hospital for their valuable help during the MRI data collection and Mr. James E. Koch, from Ryerson University, for his extensive help in design and implementation of hardware and circuitry. Publicly available MATLAB code by Dr. D.S.Lopes was used for implementation of PM algorithm. We should also thank CIHR (grant number: 111253) for funding this research.

References

[1] Joy, M., Scott, G., & Henkelman, M. (1989). In vivo detection of applied electric currents by magnetic resonance imaging. Magnetic resonance imaging, 7(1), 89-94.

[2] Eyuboglu, M., Reddy, R., & Leigh, J. S. (1998). Imaging electrical current density using nuclear magnetic resonance. Elektrik, 6, 201-14.

[3] Scott, G. C., Joy, M. L. G., Armstrong, R. L., & Henkelman, R. M. (1991). Measurement of nonuniform current density by magnetic resonance. Medical Imaging, IEEE Transactions on, 10(3), 362-374.3

[4] Perona, P., & Malik, J. (1990). Scale-space and edge detection using anisotropic diffusion. Pattern Analysis and Machine Intelligence, IEEE Transactions on, 12(7), 629-639.

[5] Schenck, J. F. (1996). The role of magnetic susceptibility in magnetic resonance imaging: MRI magnetic compatibility of the first and second kinds. *Medical physics*, *23*(6), 815-850.

[6] Seo, J. K., Yoon, J. R., Woo, E. J., & Kwon, O. (2003). Reconstruction of conductivity and current density images using only one component of magnetic field measurements. Biomedical Engineering, IEEE Transactions on, 50(9), 1121-1124.

[7] Lee, C. O., Jeon, K., Ahn, S., Kim, H. J., & Woo, E. J. (2011). Ramp-preserving denoising for conductivity image reconstruction in magnetic resonance electrical impedance tomography. Biomedical Engineering, IEEE Transactions on, 58(7), 2038-2050.

[8] Park, C., Lee, B. I., & Kwon, O. I. (2007). Analysis of recoverable current from one component of magnetic flux density in MREIT and MRCDI. Physics in medicine and biology, 52(11), 3001.

[9] Beravs, K., White, D., Serša, I., & Demsar, F. (1997). Electric current density imaging of bone by MRI. Magnetic resonance imaging, 15(8), 909-915.

[10] Yoon, R. S., DeMonte, T. P., Hasanov, K. F., Jorgenson, D. B., & Joy, M. L. (2003). Measurement of thoracic current flow in pigs for the study of defibrillation and cardioversion. Biomedical Engineering, IEEE Transactions on, 50(10), 1167-1173.

[11] Firbank, M. J., Coulthard, A., Harrison, R. M., & Williams, E. D. (1999). A comparison of two methods for measuring the signal to noise ratio on MR images. Physics in medicine and biology, 44(12), N261.

[12] Serša, I., Beravs, K., Dodd, N. J., Zhao, S., Miklavčič, D., & Demsar, F. (1997). Electric current density imaging of mice tumors. Magnetic resonance in medicine, 37(3), 404-409.

[13] Gudbjartsson, H., & Patz, S. (1995). The Rician distribution of noisy MRI data. Magnetic Resonance in Medicine, 34(6), 910-914.

[14] Foomany, F. H., Beheshti, M., Magtibay, K., Masse, S., Foltz, W., Sevaptsidis, E., ... & Umapathy, K. (2013, July). Analysis of reliability metrics and quality enhancement measures in current density imaging. In Engineering in Medicine and Biology Society (EMBC), 2013 35th Annual International Conference of the IEEE (pp. 4394-4397). IEEE.

[15] Scott, G. C., Joy, M. L. G., Armstrong, R. L., & Henkelman, R. M. (1992). Sensitivity of magnetic-resonance current-density imaging. Journal of Magnetic Resonance (1969), 97(2), 235-254.

[16] DeMonte, T. P., Wang, D., Ma, W., Gao, J. H., & Joy, M. (2009, September). In-vivo measurement of relationship between applied current amplitude and current density magnitude from 10 mA to 110 mA. In Engineering in Medicine and Biology Society, 2009. EMBC 2009. Annual International Conference of the IEEE (pp. 3177-3180). IEEE.

[17] Schenck, J. F. (1996). The role of magnetic susceptibility in magnetic resonance imaging: MRI magnetic compatibility of the first and second kinds. *Medical physics*, *23*(6), 815-850.

[18] Griffiths, D. J., & Reed College. (1999). Introduction to electrodynamics (Vol. 3). Upper Saddle River, NJ: prentice Hall.

[19] Golub, G. H., & Van Loan C. F. (2012). Matrix Computations. Baltimore, MD: JHU Press.